

**NEW CONSTRAINTS ON THE ARGON ISOTOPIC COMPOSITION OF THE MARTIAN ATMOSPHERE OVER THE PAST THREE MILLION YEARS.** W. S. Cassata<sup>1</sup>, B. E. Cohen<sup>2,3</sup>, D. F. Mark<sup>2,4</sup>, M. R. Lee<sup>3</sup>, C. L. Smith<sup>5</sup>, D. L. Shuster<sup>6,7</sup>

<sup>1</sup>Lawrence Livermore National Laboratory, 7000 East Avenue (L-235), Livermore, CA 94550 (cassata2@llnl.gov)

<sup>2</sup>Scottish Universities Environmental Research Centre (SUERC), Rankine Avenue, East Kilbride, G75 0QF, UK

<sup>3</sup>School of Geographical and Earth Sciences, The University of Glasgow, G12 8QQ, UK

<sup>4</sup>Department of Earth & Environmental Science, University of St Andrews, KY16 9AJ, UK

<sup>5</sup>Department of Earth Sciences, The Natural History Museum, London SW7 5BD, UK

<sup>6</sup>Department of Earth and Planetary Science, University of California, Berkeley, CA 94720-4767, USA

<sup>7</sup>Berkeley Geochronology Center, 2455 Ridge Road, Berkeley, CA 94709, USA

**Introduction:** Shock melt veins and minerals in Martian meteorites contain trapped atmospheric gases that reflect the isotopic, and occasionally elemental, composition of the atmosphere at the time of their incorporation [1-3]. As such, measurements of trapped atmospheric gases in meteorites that differ in age can be used to reconstruct paleoatmospheric conditions on Mars and are useful for studying the dynamic relationship between atmospheric evolution and planetary outgassing [e.g., 4-7]. The composition of the modern Martian atmosphere constrains the end-point of all inverse-forward models of Martian atmospheric evolution. Therefore, determining the composition of the modern Martian atmosphere to high precision is important.

Measurements of modern atmospheric argon (Ar) by the Curiosity rover and in young Shergottites yield indistinguishable results within uncertainties [8-11]. However, uncertainties at the >5-10% level still exist due to instrumental limitations (in the case of the *in situ* rover measurements) and inter-sample variations in the inferred composition of the atmospheric component (in the case of laboratory meteorite measurements; see review by [8]). Some variation between laboratory measurements likely results from uncertainties in applying cosmogenic corrections, which require simplifying assumptions regarding the spatial homogeneity of target elements for cosmogenic production and the distribution of cosmogenic nuclides relative to trapped and reactor-derived Ar isotopes [12]. Cassata and Borg [12] developed a new cosmogenic correction approach that utilizes step-wise cosmogenic Ar production rate estimates to mitigate uncertainties associated with the assumption described above. In an effort to improve the precision with which the modern Martian atmospheric Ar isotopic composition is determined, this new approach was applied to detailed <sup>40</sup>Ar/<sup>39</sup>Ar step-heating experiments conducted on a suite of Shergottites.

**Samples and Methods:** <sup>40</sup>Ar/<sup>39</sup>Ar experiments conducted on Martian meteorites to obtain accurate age constraints generally involve degassing samples at lower-resolution (e.g., <20 extractions per aliquot). To more adequately resolve trapped components retained within different phases, detailed incremental heating

schedules designed to isolate the release of noble gases from individual host minerals according to their diffusion kinetics are beneficial. To facilitate these experiments, diode and CO<sub>2</sub> laser heating techniques are useful. The diode laser heating approach combines the benefits of conventional furnace heating (homogeneous temperature) with low blanks typical of laser heating. The low blanks further enable the use of tightly spaced temperature increments that release less gas per step.

To this end, detailed diode and CO<sub>2</sub> laser heating experiments were conducted on Shergottite whole-rock fragments, mineral separates, and impact melt separates at Lawrence Livermore National Laboratory, the Scottish Universities Environmental Research Centre, and the Berkeley Geochronology Center. The discussion that follows focuses on data obtained from Northwest Africa (NWA) 6963 and two Shergottites that have previously been shown to contain a high concentration of trapped Martian atmosphere, Tissint [e.g., 13] and Elephant Moraine (EETA) 79001 [e.g., 8]. EETA 79001 crystallized at ~170 Ma [14], has a cosmic ray exposure (CRE) age of ~0.7 – 0.9 Ma [e.g., 15], and contains abundant impact melt. Tissint crystallized at ~575 Ma [16], has a comparable CRE age of ~1.1 Ma [17], and likewise contains abundant impact melt as a result of shock heating. We are not aware of constraints on the crystallization or exposure age of NWA 6963, although the meteorite is chemically and petrographically similar to Shergotty, which has a crystallization age of ~165 Ma [14] and CRE age of ~2.5 – 3.0 Ma [e.g., 18,19]. NWA 6963 also contain impact melt as a result of shock heating.

**Results and Discussion:** Figure 1 depicts inverse isochron diagrams obtained from the incremental heating of whole-rock and glass fragments of EETA 79001, Tissint, and NWA 6963. All data were corrected for cosmogenic <sup>36</sup>Ar following procedures described in Cassata and Borg [12] using <sup>38</sup>Ar exposure ages of  $0.9 \pm 0.1$ ,  $1.1 \pm 0.1$ , and  $2.7 \pm 0.3$  Ma, respectively. The resulting trapped <sup>40</sup>Ar/<sup>36</sup>Ar ratios inferred from the inverse isochron diagrams are shown in Figure 1. By inspection it is clear that all three Shergottites yield statistically indistinguishable trapped <sup>40</sup>Ar/<sup>36</sup>Ar ratios.

The trapped  $^{40}\text{Ar}/^{36}\text{Ar}$  ratios are also indistinguishable from several previously reported values obtained from Shergottites (e.g., EETA 79001 =  $1735 \pm 85$  [20]; Allan Hills 77005 =  $1760 \pm 100$  [20]; Tissint =  $1714 \pm 170$  [13]) and that determined by the Curiosity rover ( $1900 \pm 300$  [10]). Collectively, these measurements indicate that the Ar isotopic composition of the Martian atmosphere has been stable from  $\sim 3$  Ma (the assumed ejection age of NWA 6963) to the present. These Shergottite data further provide the highest precision estimate of the modern Martian atmospheric  $^{40}\text{Ar}/^{36}\text{Ar}$  ratio.

Our analysis of the trapped  $^{38}\text{Ar}/^{36}\text{Ar}$  ratios in EETA 79001, NWA 6963, and Tissint is on-going. At the conference,  $^{38}\text{Ar}/^{36}\text{Ar}$  results from these samples will be presented. The implications of a more precise determination of the isotopic composition of Martian atmospheric Ar for modeling atmospheric evolution and planetary outgassing will be discussed.

**References:** [1] Bogard, D.D. and Johnson P. (1983) *Science*, 221, 651-654. [2] Becker R.H. and Pepin R.O. (1984) *EPSL*, 69, 225-242. [3] Bogard D.D. et al. (1989) *Meteoritics*, 24, 113-123. [4] Hutchins K.S. and Jakosky B.M. (1996) *JGR: Planets*, 101, 14933-14949. [5] Cassata W.S. et al. (2012) *Icarus*, 221, 461-465. [6] Cassata W.S. (2017) *EPSL*, 479, 322-329. [7] Kurokawa H. et al. (2018) *Icarus*, 299, 443-459. [8] Bogard D.D. et al. (2001) *SSR*, 96, 425-458. [9] Wiens R.C. et al. (1986) *EPSL*, 77, 149-158. [10] Mahaffy P.R. et al. (2013) *Science*, 6143, 263-266. [11] Atreya S.K. et al. (2013) *GRL*, 40, 5605-5609. [12] Cassata W.S. and Borg L.E. (2016) *GCA*, 187, 279-293. [13] Avicé G. et al. (2018) *GPL*, 6, 11-16. [14] Nyquist L.E. et al. (2001) *Chronology and Evolution of Mars*, 96, 105-164. [15] Pal D.K. et al. (1986) *GCA*, 50, 2405-2409. [16] Brennecka G.A. et al. (2014) *M&PS*, 49, 412-418. [17] Nishiizumi K. et al. (2012) *75<sup>th</sup> MetSoc*, Abstract #5349. [18] Eugster O. et al. (2002) *M&PS*, 37, 1345-1360. [19] Bogard D.D. et al. (1984) *GCA*, 48, 1723-1739. [20] Bogard D.D. and Garrison D.H. (1999) *M&PS*, 34, 451-473.

**Acknowledgments:** This work performed under the auspices of the U.S. Department of Energy by Lawrence Livermore National Laboratory under Contract DE-AC52-07NA27344. Financial support at LLNL was provided by NASA (grant NNH14AX56I to W.S.C.) and an LLNL Laboratory Directed Research and Development project (17-ERD-001) and to SUERC via the UK STFC (grant ST/K000918/1 to D.F.M and M.R.L.). Ben Weiss is thanked for providing sample EETA 79001 to W.S.C. and D.L.S. The Natural History Museum London is thanked for providing Tissint to B.E.C., D.F.M., and M.R.L. (loan BM.2012,M3).

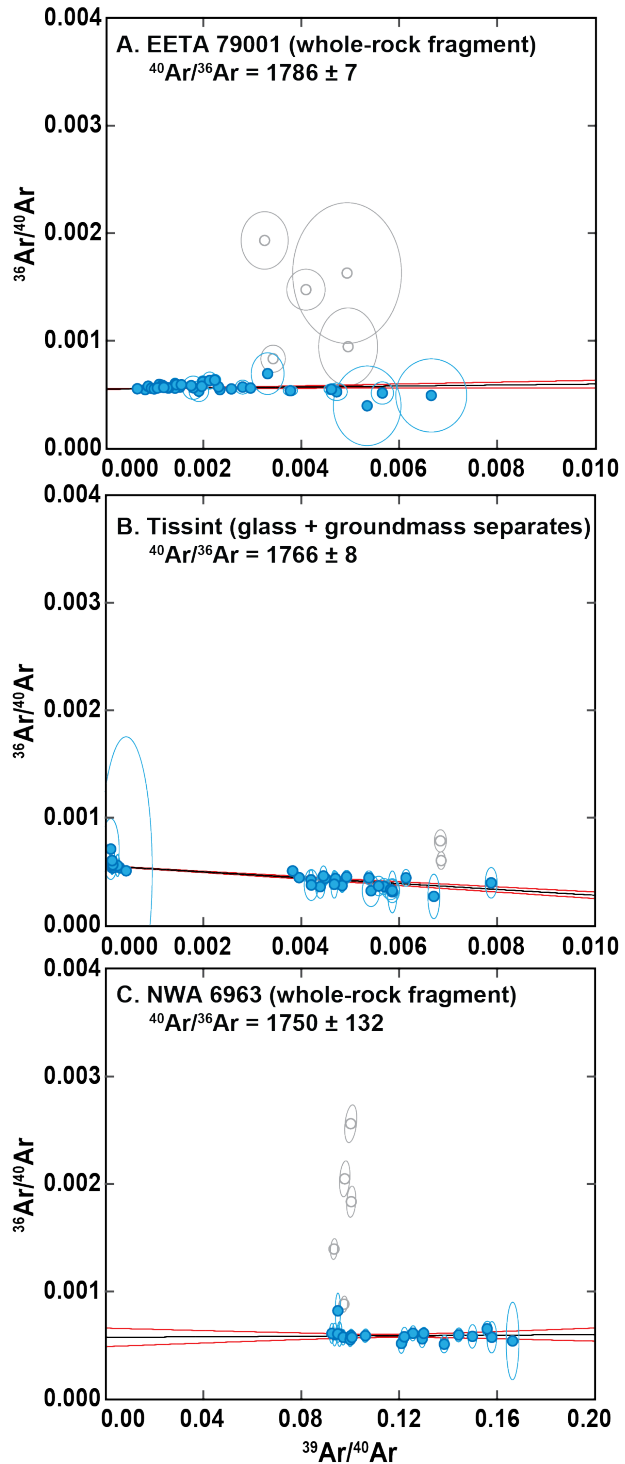


**Figure 1:**  $^{40}\text{Ar}/^{39}\text{Ar}$  inverse isochron diagrams. Error ellipses reflect the uncertainty correlation and  $\pm 2\sigma$  analytical uncertainties. The confidence intervals on the isochron regressions (red lines) are shown at 2 S.E. Trapped  $^{40}\text{Ar}/^{36}\text{Ar}$  ratios are listed at 1 S.E. Gray symbols are derived from low-T extractions and were excluded from isochron regressions. To improve the clarity of the figure, additional data points with significantly larger uncertainties were excluded.